Chemical ordering in the first stages of Co-Pt film growth on Pt(111)

M. De Santis,* R. Baudoing-Savois, P. Dolle, and M. C. Saint-Lager
Laboratoire de Cristallographie, CNRS, associé à l'Université J. Fourier et à l'INPG, Boite Postale 166 X, 38 042 Grenoble cédex 9, France

(Received 22 March 2002; published 15 August 2002)

The first stages of the growth of Pt_CCo_{1-C} films on Pt(111) were investigated *in situ* by x-ray reflectometry and grazing incidence x-ray diffraction. Co-Pt ultrathin alloys are among the most interesting candidates for magneto-optic recording media. In this study we show that, at a given substrate temperature, a surface-induced equilibrium state is established since the very beginning, resulting in a bilayer where Pt segregates on top of a Co-rich buried layer. The sample obtained by codeposition of about 1 monolayer $Pt_{20}Co_{80}$ at 520 K was studied in details. Its structure was solved by quantitative analysis of the intensity distribution of crystal truncation rods. The outermost plane contains at least 80 at. % Pt, while the buried one is Co rich, with a concentration that is also close to 80%. No significant Co diffusion in the underlying substrate layers was observed. The stacking was found fcc in coherent continuation with the substrate. We believe that the growth mechanism observed here is responsible for clustering in Pt-rich films with perpendicular magnetic anisotropy.

DOI: 10.1103/PhysRevB.66.085412 PACS number(s): 68.55.−a, 61.10.−i, 75.70.−i, 81.15.Aa

I. INTRODUCTION

For about 10 yr Pt_CCo_{1-C} alloys have attracted a great interest as an alternative to the artificially modulated Pt/Co superlattices for the future generation of magneto-optical recording media.[1–4] Alloy films exhibit properties analogous to those of the corresponding multilayers, i.e., large perpendicular magnetic anisotropy (PMA) and coercivity, Kerr rotation enhancement at blue wavelengths and high resistance to oxidation and corrosion. They have the advantage to be more easily manufactured. This improvement of the magnetic properties with respect to bulk alloys was observed both for Co-rich and for Pt-rich compositions provided that the growth is performed in a well-defined temperature range.

The Pt-Co phase diagram exhibits $L1_2$ and $L1_0$ order at about Pt_3Co and PtCo composition, respectively,[5] with a transition to disordered fcc above 1000 K (1100 K) for Pt_3Co (PtCo). A $L1_2$ phase was also predicted for $PtCo_3$.[6] Both $L1_2$ and $L1_0$ phases yield the same composition for all the (111) planes. A martensitic transition from fcc to (disordered) hcp is observed below 650 K for a Co content greater than 85 at. %.

Harp *et al.*[3] produced $PtCo_3$ thin hcp films by coevaporation on (0001) sapphire. These films are (0001) oriented and show a new phase with chemical modulation along the growing direction. The best samples were obtained by keeping the substrate between 600 and 650 K during evaporation, and partial long-range order (LRO) was observed for films produced at temperatures as low as 500 K. These films exhibited PMA that was correlated to LRO and was explained by the presence of ''inner interfaces'' in a similar way as in Co/Pt multilayers. Similar results were also obtained by Maret *et al.*[7]

The explanation of the magnetic properties of Pt-rich films and their correlation with the atomic structure is more problematic. $Pt_{75}Co_{25}$(111) fcc films, grown in the same temperature range as Co-rich films, show a large magnetic anisotropy[1] and an increase in the Curie temperature and of the magnetization,[8,9] but no new phase was observed in contrast to the case of $PtCo_3$. It was only established that the appearance in these films of $L1_2$ ordering reduces the Curie temperature to the value expected of the corresponding bulk alloy. The improvement of the magnetic properties was explained by Co clustering.[8] It is well known that Pt_CCo_{1-C}(111) bulk alloys show Pt segregation at the surface and an oscillating Pt concentration profile in the underlying layers.[10–12] It was therefore suggested that Co platelets form as a surface-driven-growth effect in Pt-rich films during codeposition.[9] A surface equilibrium state induced by Pt segregation would be trapped in the film during growth. Two different extended x-ray-absorption fine structure studies on $Pt_{\sim 75}Co_{\sim 25}$ films, grown at 570 and 690 K, respectively, were performed to investigate the local chemical order. In the first one a very small anisotropy was found.[13] On the opposite, in the second experiment[14] the distribution of first neighbors was found to be significantly different for atoms lying in the same layer or in the adjacent ones. The resulting picture was a preference for homoatomic pairs in the (111) plane, balanced with preferential heteroatomic pairs out of the plane.

In this paper we discuss the first stages of the growth of Pt_CCo_{1-C}/Pt(111) films. Section II is devoted to experimental details. In Sec. III the x-ray reflectivity measured during the growth is discussed. In Sec. IV, we solve the structure of a film, obtained by codeposition at 520 K of about 1 monolayer (ML) of alloy with a nominal composition of $Pt_{20}Co_{80}$, by means of quantitative analysis of surface x-ray diffraction (SXRD) data.

II. EXPERIMENT

The measurements were carried out on the surface x-ray diffraction setup of the BM32 beam line[15] at the European Synchrotron radiation facility (ESRF). It consists of an UHV chamber mounted on a *z*-axis diffractometer.[16]

The Pt(111) crystal (mosaicity$<0.05°$, miscut$<0.2°$) was previously annealed in about 10^{-6} mbar O_2 to eliminate carbon. It was then cleaned by repeated cycles of Ar^+ sputtering

and annealing at about 1100 K. Sample cleanliness was checked by Auger spectroscopy.

Cobalt and platinum were coevaporated from high-purity rods by electron bombardment. The base pressure was 2×10^{-10} mbar, rising up to 4×10^{-10} mbar during evaporation. Films with the nominal composition $Pt_{20}Co_{80}$ were evaporated at rates of 0.025 and 0.1 ± 0.02 ML/min for Pt and Co, respectively. For the other samples, the Co rate was adjusted to the desired composition, the Pt rate being constant. The Pt rate was derived from the x-ray reflectivity during Pt/Pt(111) growth at 510 K. This temperature was chosen to ensure a layer-by-layer growth mode.[17] The Co evaporation was calibrated by studying the reflectivity of a ''thick'' $Pt_{20}Co_{80}$ film codeposited at 540 K. The period of Kiessig fringes gave a thickness of 13 ML. It was assumed that bulk diffusion is negligible at this temperature, as confirmed in the following. This is consistent with previous measurements showing the onset of bulk diffusion beyond 650 K for Co/Pt(111) ultrathin films deposited at room temperature (RT).[18]

The measurements were carried out at 18 keV photon energy, except for the data of Fig. 1 curve *B* and Fig. 3 taken at 11 keV. Off-specular diffraction rods were measured at grazing incidence (1.74°). A hexagonal unit cell was taken for the Pt(111) crystal with $\boldsymbol{a}$ and $\boldsymbol{b}$ vectors in the surface plane and $\boldsymbol{c}$ perpendicular to it. The interlayer spacings are $d_{Pt}=2.266$ Å and $d_{Co}=2.03$ Å for bulk Pt(111) and bulk Co(0001), respectively, with $|\boldsymbol{c}|=3d_{Pt}$. The hexagonal indices read $H=(k-h)/2$, $K=(l-k)/2$, and $L=h+k+l$, where h, k, and l are the cubic ones (see Ref. 19). In the reciprocal space, Bragg conditions occur with a periodicity $\Delta L=3$ along the crystal truncation rods, which are perpendicular to the surface. During deposition, data were collected in antiphase conditions (L about 1.5 on the specular rod) to maximize the surface sensitivity.

The data reduction and the structural analysis were performed using the ''ANA-ROD'' package,[20,21] written by Vlieg. The (*HKL*) intensities were measured by scanning the sample azimuth (the polar angle for the specular rod). The data were integrated after background subtraction, and the structure factors were then calculated by applying the Lorentz correction and the correction factors for the beam polarization and the illuminated area of the sample.[22] The same scale factor was applied to all rods.

The anomalous correction for the Pt scattering factor was included in the data analysis ($f'_{Pt}=-2.2$ electrons at 18 keV).[23]

III. X-RAY REFLECTIVITY DURING THE GROWTH

In a layer-by-layer growth of Pt/Pt(111), the specular reflectivity in antiphase conditions oscillates with a period of 1 ML.[24] Curve *A* of Fig. 1 illustrates the measurements (at $L=1.52$) used for the calibration of the source. The observed decrease between the values at 0 and 1 ML is due to roughness. Following Robinson,[25] we find that $\beta=0.14$, where β describes the surface roughness with respect to the bulk termination.

Curve *B* represents the reflectivity, measured in a previous experiment, during the growth of Co/Pt(111) at RT.[18] In this case the first maximum is obtained after 2-ML deposition.[26,24] Its intensity is reduced compared to the bare substrate, which is also due to surface roughness. This measurement and those discussed later on were performed at $L=1.6$. This choice corresponds to a scattering vector q, which satisfies the relationship $qd=\pi$ for an interlayer distance d of 2.12 Å, approximately at mid-distance between d_{Pt} and d_{Co}.

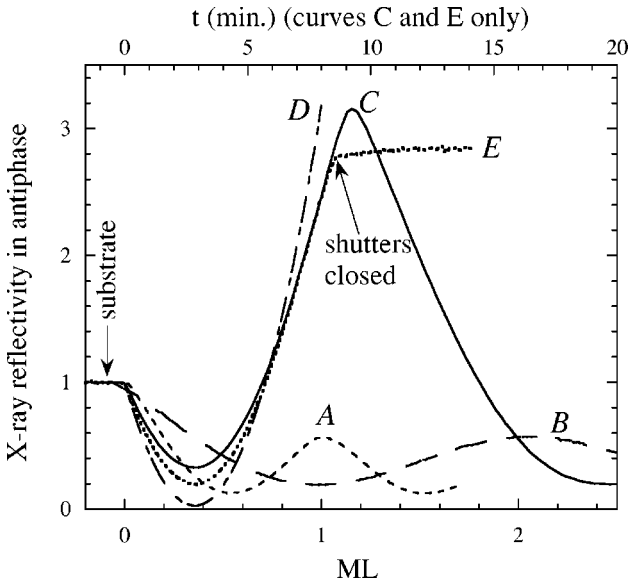

FIG. 1. X-ray reflectivity close to antiphase condition during deposition. *A*: Pt/Pt(111) at 510 K. *B*: Co/Pt(111) at RT. *C*: 13 ML $Pt_{20}Co_{80}$ at 540 K (only shown up to 2.5 ML). *D*: simulation in the framework of model (c) (see Fig. 2). *E*: 1 ML $Pt_{20}Co_{80}$ at 520 K (the evaporator shutters were closed after 8.5 min). The intensity was measured at $L=1.52$ for homoepitaxy and at $L=1.6$ in the other cases. It is normalized to the clean substrate reflectivity.

Curve *C* shows the reflectivity during the codeposition at 540 K of 13 ML of a surface alloy with a nominal composition $Pt_{20}Co_{80}$ (only shown here up to 2.5 ML). The growth looks very different from the simple quasi layer-by-layer mode. The most striking feature is the strong peak centered at about 1 ML (1.15 ± 0.2 ML). At the maximum, the diffracted intensity increases by a factor of $R=3.15$ compared to the clean substrate. A bilayer growth is the simplest process to explain this behavior. The top layer should be Pt rich and the underlying one Co rich. In this framework, the maximum occurs at the completion of the bilayer. This bilayer growth is promoted by an interlayer transport and/or exchange mechanism, which involves substrate atoms. The extraction of the layer-by-layer composition from the reflectivity in antiphase requires the knowledge of the surface roughness. We suppose in the following that the surface is flat and that the interface with the substrate is sharp. These hypotheses about the thickness and the abruptness of the surface layer will be confirmed by the structural analysis in the following section. The reflectivity of the full bilayer calculated at $L=1.6$ is a simple generalization of the formula given in Ref. 24. We obtain

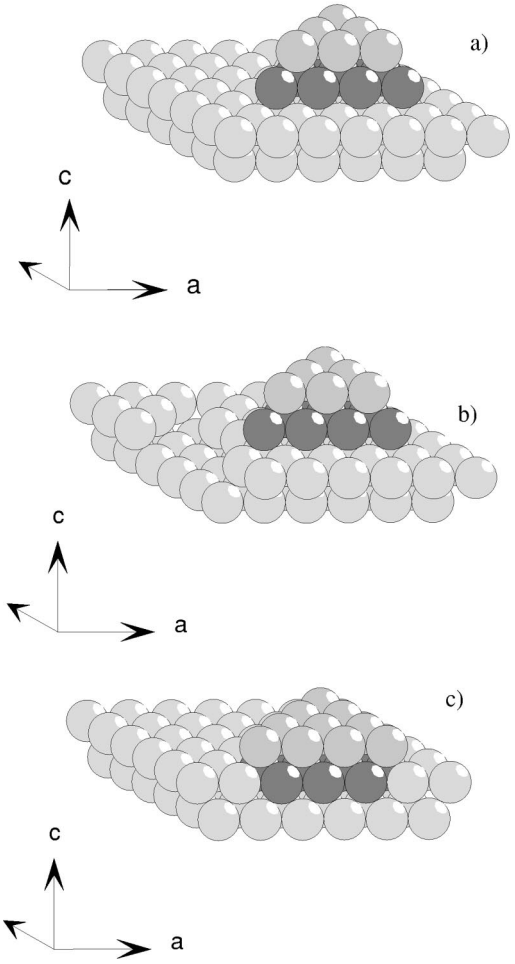

FIG. 2. Models of bilayer growth. (a) on top of the surface, (b) with the appearance of pits, (c) by exchange with substrate Pt atoms.

$$R=\left|1+\frac{(C_2-C_1)(f_{\mathrm{Pt}}-f_{\mathrm{Co}})}{F_{\mathrm{Pt}}}\right|^2.$$

Here $F_{\mathrm{Pt}}=f_{\mathrm{Pt}}/(1-e^{-iqd_{\mathrm{Pt}}})$ is the substrate structure factor, f_{Pt} (f_{Co}) is the Pt (Co) atomic scattering factor,[27] C_2 is the Pt fraction in the top layer, and C_1 that one in the underlying layer (see Fig. 5). This relationship is obtained with interlayer distances of 2.12 Å (close to the optimum values of Table I). The intensity is normalized to the clean substrate one. Inserting the experimental value $R=3.15$, we find $C_2-C_1=0.6$. The situation is thus the following: (1) We have codeposited about 1 ML ($Pt_{20}Co_{80}$); (2) A two-layer-thick film has grown, as shown by the increase in the reflectivity in antiphase; (3) Layer 2 (the outermost one) is Pt rich ($C_2-C_1=0.6$); and (4) Layer 1 (at the interface) is Co rich. Since only 0.2 ML Pt were evaporated, Pt atoms present in the top layer are coming mainly from the substrate. This means that exchange occurs between the deposited atoms and those of the substrate top layer.

In Fig. 2 we sketch three simple growth models:

(a) A bilayer formed on top of the substrate with Pt from an ''inner source.''

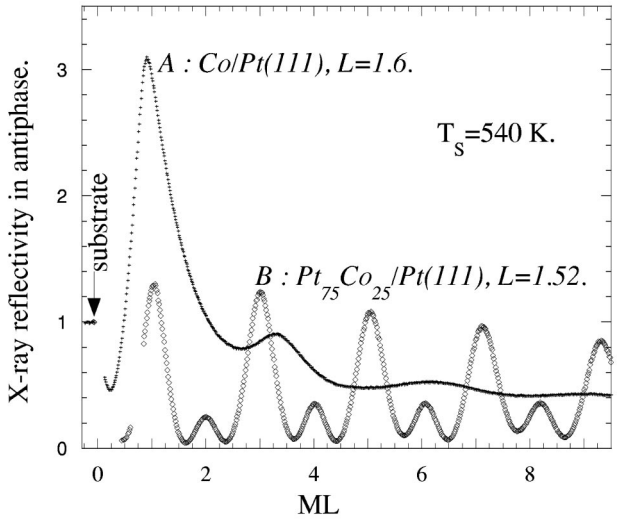

FIG. 3. Reflectivity during deposition at 540 K of Co/Pt(111) (curve *A*) and $Pt_{75}Co_{25}$ Pt(111) (curve *B*). It was measured at $L=1.6$ and $L=1.52$, respectively (missing points correspond to x-ray shutter closures).

(b) Pt/Co islands resulting from Pt substrate atoms moving on top of adatoms, and leaving pits in the surface.

(c) Co atoms directly incorporated in the substrate layer by exchange with Pt atoms that form an adlayer.

Model (a) would result in a continuous increase of the intensity diffracted in antiphase. Model (b) would give quite rough a surface, with a quick decrease of the intensity: this is in clear contradiction with Fig. 1. Model (c) corresponds quite well to the experimental intensity, which decreases first and then increases. This latter model is shown as curve *D* in Fig. 1. However, in a subsequent experiment performed under similar conditions, the minimum in curve *C* was less pronounced. The reflectivity was hence in between what is expected for models (a) and (c). It looks like these two growth mechanisms can coexist in some cases, their weight depending either on the deposition rate or on less controlled parameters such as step density, surface defects, and fluctuations in the substrate temperature.

Pt segregation at 540 K was observed for a large range of flux compositions. Even for pure Co evaporation the reflectivity reaches a similar intensity ($R\sim3.1$) at about the same Co amount (curve *A* in Fig. 3). It can be inferred that the initial growth for pure Co leads to a similar bilayer.

For $Pt_{75}Co_{25}$ the first oscillation is much less pronounced, yielding $C_2-C_1\sim0.11$ ML. Then the growth turns to an almost perfect layer-by-layer mode. The small decrease of the oscillation amplitude denotes both a sharp interface and a flat surface, which means that diffusion of Co into the bulk is unlikely under these growth conditions.

IV. BILAYER STRUCTURE

As it is well known,[25] a semi-infinite crystal gives rise to a characteristic x-ray diffraction intensity distribution versus the momentum transfer perpendicular to the surface, which is

called crystal truncation rod (CTR). In both directions parallel to the surface, sharp peaks are observed, when the in-plane Bragg conditions are fulfilled. A film in coherent epitaxy modifies the intensity distribution along the CTR's. A full surface structure determination requires the measurement of the diffracted intensity along several CTR's.

A fresh film was grown with the nominal composition $Pt_{20}Co_{80}$ as for *C* (Fig. 1) but evaporation was stopped just before the bilayer completion (Fig. 1 curve *E*, $T=520$ K instead of 540 K). Data were collected at RT for structural analysis. No additional surface rods were observed by scanning the in-plane component of the scattering vector *q*, which indicates that the Co atoms are in site.

The (10), (01), and (11) CTR's, their respective equivalents $(\bar{1}1)$, $(1\bar{1})$, and $(\bar{1}\bar{1})$, and the (00) rod were measured. A total of 294 reflections were collected, 177 of which being nonequivalent. The average agreement factor of the 109 equivalent ones was quite good ($\varepsilon=0.031$). The data are plotted in Figs. 4(a), 4(b), and 4(c), together with the related error bars. The $(01L)$ rod was converted into the $(10\bar{L})$ one by symmetry.

A sketch of the surface model employed is shown in Fig. 5. It consists of a bilayer on top of the substrate, and it comes out quite intuitively looking at the data. The film thickness is deduced directly from the width of the surface peaks. In the growth of a close-packed arrangement there are three sites that can be occupied, and therefore two ways to pile up an atomic plane over the free surface. In our overlayer model the stacking follows the bulk fcc sequence (...*ABCABC*). Indeed a twinned fcc domain with stacking ...*ABCACB* or a hcp arrangement (...*ABCACA* or ...*ABCABA*) would result in completely different positions of the surface peaks along the (10) rod.

The data were fitted using a χ^2 minimization.[20] We modeled the film as a bilayer in coherent epitaxy, with bulk stacking sequence. The positions and the chemical compositions of both atomic planes were optimized. A unique but anisotropic Debye parameter was introduced, which incorporates the structural disorder too. The substrate top-layer position and its Debye-Waller factor (anisotropic) were also fitted. Finally we optimized the fraction of film covering the surface (S_f). The fitted rod profiles are plotted as solid curves in Fig. 4. The final model gives a χ^2 of 2.8 (and an *R*-factor of 0.05). The best-fit parameters are listed in Table I. The Pt concentration is 80 at. % in the top layer and 22 at. % in the buried one, in good agreement with the results of the previous section. There is also a good agreement between the fit results and the evaporated Co amount. The best fit gives $[(1-C_1)+(1-C2)]S_f=0.91$ ML of Co in the bilayer, which has to be compared to 0.85 ± 0.17 ML of Co evaporated according to the source calibration. Interlayer distances of 2.11 and 2.10 Å were found for d_{01} and d_{12}, respectively, while the in-plane distance is 2.78 Å due to coherent epitaxy. This gives a bond length of 2.64 Å (2.65 Å) between atoms in layer 2 (1) and atoms in layer 1 (0). Here 2, 1 and 0 label the top layer, the underlying one, and the substrate outermost plane, respectively. In the $L1_0$ bulk phase, Co atoms have eight Pt first neighbors at 2.65 Å and four Co first neighbors

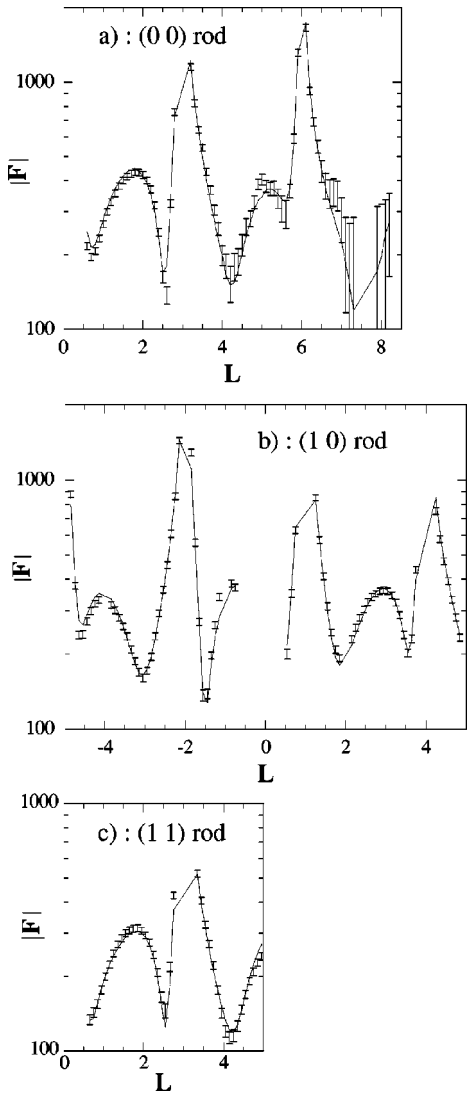

FIG. 4. Experimental structure factors (with error bars) and best fit (full lines) along the (0 0) rod (a), the (1 0) rod (b), and the (1 1) rod (c).

at 2.70 Å,[28] a difference that comes from the tetragonal distortion. In the sample under study the majority of Co-Co bonds are parallel to the surface plane, while the Co-Pt ones are mainly oriented out of plane, a consequence of the chemical profile. The volume per Co atom is increased compared to bulk PtCo, the difference coming from the substrate-induced strain.

Co diffusion in layer 0 was considered. The best fit gave a

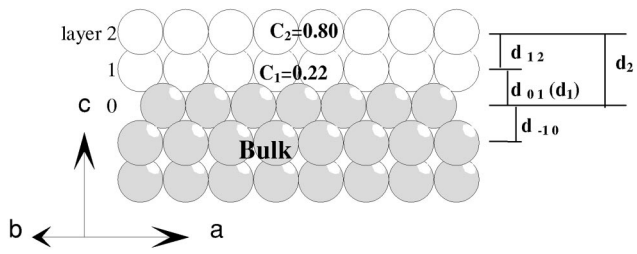

FIG. 5. Sketch of the bilayer model structure.

TABLE I. Best-fit values for the ~1 ML $Pt_{20}Co_{80}$ film. In brackets the result with vacancies in the top layer.

n	$d_{n-1,n}$ (Å)	O_n (Pt)	C_n (Pt)	$\overline{u_x}, \overline{u_y}$ (Å)	$\overline{u_z}$ (Å)	S_f
Bulk	2.266			0.063	0.063	
0	2.300±0.001	1	0.98±0.02	0.084±0.003	0.090±0.004	
1	2.108±0.005	1	0.22±0.01	0.082±0.004	0.116±0.003	0.93±0.005
2	2.100±0.005	1	0.80±0.02	0.082±0.004	0.116±0.003	
		(0.93±0.07)	(0.9±0.1)			

negligible Co content in this layer (98±2 at. % Pt). A small relaxation of the $d_{-1,0}$ distance (+0.03 Å) and an increase of the Debye-Waller in layer 0 were found with respect to the Pt bulk values. Since the bilayer has mixed composition, buckling is expected. It was taken into account indirectly through an effective out of plane Debye factor in layers 1 and 2. Finally, a very good agreement was reached between the fitted S_f (0.93) and the ratio $t_d/t_M=0.92$, were t_d is the deposition time and t_M the time after which a maximum is observed in Fig. 1, curve *C*.

Up to now the surface (layer 2) was considered fully occupied (with respect to layer 1). However, it is not possible to fit separately its occupation (O_2) and the Pt concentration (C_2). When vacancies are considered in the surface layer, an increase in its Pt content is obtained. This reaches 100% Pt when $O_2=0.86$, the lowest occupation value consistent with the measurements. The result of the structural refinement would therefore be $O_2=0.93\pm0.07$, $C_2=0.9\pm0.1$. However, for a pure Pt surface, the filling of the vacancies would increase the reflectivity beyond the maximum ($R=3.15$) observed during the deposition of the 13-ML film (Fig. 1, curve *C*).

Simulations were performed for all possible stacking sequences. While the (00) and (11) rods are not sensitive at all to the stacking and show good agreement whatever the model, only the nontwinned fcc stacking (...*ABCABC*) fit the (10) rod data: all other models result in shifts of the surface peaks.

Epitaxy follows from the comparison between the specular rod and the other CTR's. The former is sensitive to the chemical profile along the growth direction, while only regions of the films with the same surface mesh of the substrate give contributions to the (11) and (10) CTR's. Since all rods were fitted with the same parameter values, we conclude that the film is in coherent epitaxy with the substrate.

In the histogram of Fig. 6, the comparison between the film under study and the layer-by-layer chemical profile at the surface of Pt-Co(111) bulk alloys with different stoichiometry is plotted. The $Pt_{80}Co_{20}(111)$ and $Pt_{25}Co_{75}(111)$ profiles are known from quantitative low-energy electron diffraction analysis.[10,12] The surface structure of the Co-rich crystal was also solved by SXRD.[11] Pt segregates at the surface of bulk alloys, with an oscillating composition profile in the underlying layers. The amplitude of the oscillation presently found for the bilayer is a little larger than for bulk alloy surfaces which, coupled with the surface strain, may have important implications for magnetism.

V. DISCUSSION AND CONCLUSION

Metal films deposited onto metal substrates can given rise, depending on the temperature, to interdiffusion limited to a few layers close to the surface and eventually to metastable surface alloys during the kinetics of dissolution.[29] In some cases the influence of the surface on the equilibrium state produces phases that are not observed in the bulk diagram, with different magnetic or catalytic properties. Perhaps the most interesting feature, at least for magnetism, is an alternated composition in layers parallel to the surface. Such a structure is rarely encountered in alloy films, which are obtained by annealing a RT deposit. It has been observed in the case of Mn/Pt(111): a surface-layered Pt/Pt_3Mn phase that has no corresponding bulk phase is obtained by annealing at 950 K a film of 10 ML.[30] In the case of Co/Pt(111), thick films (about 10 ML) are stable under annealing up to 650 K. Above this temperature a Pt-rich bulklike alloy phase forms, with the same composition for all the (111) planes.[18,31] The interdiffusion starts well below the onset of bulk diffusion[32] and seems to be related to Co hcp→fcc martensitic transition. For the Co-Pt system, a new layered alloy phase was only obtained by codeposition of Co-rich films on a heated substrate.[3] The mechanism of growth of this phase is still not completely understood.

We have shown here that codeposition of Pt_CCo_{1-C} films onto Pt(111) at 540 K results, in the first stages of growth, in

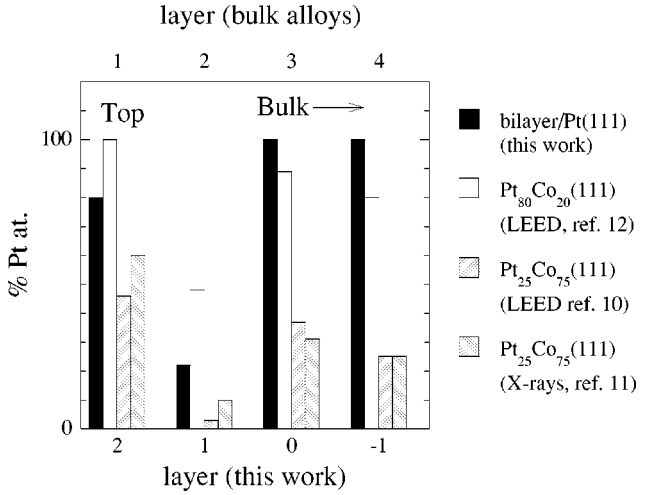

FIG. 6. Layer-by-layer composition of the ~1 ML $Pt_{20}Co_{80}$ film deposited on Pt(111) at 520 K. It is compared with the chemical profile at the surface of $Pt_{80}Co_{20}(111)$ and $Pt_{25}Co_{75}(111)$.

a template layer two atomic planes thick, which is formed by incorporating substrate atoms. The surface is Pt enriched, for flux compositions ranging from pure Co to $Pt_{75}Co_{25}$. We quantitatively studied the surface obtained after deposition of about 1 ML $Pt_{20}Co_{80}$. It results in a bilayer with an abrupt interface and a flat surface, which is in coherent epitaxy with the substrate and follows the same stacking sequence. The data analysis yields a layer-by-layer chemical profile $Pt_{80}Co_{20}/Pt_{22}Co_{78}/Pt(111)$. Since the actual parameter fitted in the data analysis is merely a scattering amplitude of each layer, there is a small uncertainty in the top layer composition: if vacancies are present, the Pt fraction of the occupied sites resulting from the fit is increased. Our findings are consistent with the chemical profile observed at the surface of (111) oriented bulk alloys,[10,11] which oscillates in composition over the first three atomic layers. A similar bilayer structure was also found by annealing at 573 K a film of 1 ML Co/Pt(111).[33]

The preference of the deposited metal to be located in the second layer, covered by substrate atoms, was observed or predicted in many systems (Refs. 34 and 35, and references cited therein). Most of them present a strong tendency to phase separation and surface energies favoring the substrate segregation. However, subsurface growth happens also in the case of miscible metals, forming eventually ordered structures. Two interesting examples are the Au/Ag(110) system[36,37] and the Pd/Cu(110) one.[38] In the last case a Cu termination on top of an ordered PdCu layer was observed at 0.5 ML coverage. This yields the same structure as for the Cu_3Pd $L1_2$ alloy over the first three atomic planes. The top layer is formed partly by Cu atoms expelled during alloying, partly by substrate material supplied from steps and terraces. This results in a very rough morphology [model (b) in Sec. III].

Alloying in the surface layer was also recently observed for submonolayer growth of Ni on vicinal Pt(111).[39] Although Ni atoms are incorporated preferentially at step sites, a few exchange processes on terraces take place even at low temperature (150 K). The absence of stacking faults and the nucleation of Pt islands attached to the step edges indicate that Ni atoms expel Pt atoms from the surface layer. This growth mode via substitution of substrate top layer atoms with the evaporant ones is similar to our observation [model (c) in Sec. III]. For submonolayer Co/Pt(111) films deposited at room temperature a small amount of Co atoms incorporated into the Pt surface was also observed.[40] However, in our experiment most of the surface substrate atoms are substituted.

We think that the same growth process discussed in this paper is responsible for 2D Co clustering in Pt-rich thick films deposited at about 600 K. This was proposed to explain their magnetic properties,[8,9] in the absence of a layered crystallographic phase. The surface structure described in Sec. IV seems very promising for magnetic studies, and a large PMA is expected due to its layered and strained structure, and to the sharpness of its interfaces. A large enhancement in the polar magneto-optical Kerr effect (MOKE) has already been observed in two similar artificial structures. (a) An ultrathin Co wedge grown on Pt(111) and capped with a Pt overlayer showed a thickness-dependent PMA, with a peak in the coercivity at 1.5 ML Co.[41] In this case the growth at RT should result in a quite rough interface, which is a drawback since roughness plays a crucial role with respect to the hysteresis properties of ferromagnetic ultrathin films.[42] (b) The second sample was 1 ML Co/Pt(111) annealed at about 710 K.[43] In this case the enhancement in the Kerr signal was explained with the formation of a Co-Pt alloy, but a full structural analysis was missing. Recently MOKE measurements on Co/Pt(111) films of thickness 1 and 2 ML, deposited at 540 K, were performed. They showed square and large hysteresis loops.[44]

ACKNOWLEDGMENTS

We acknowledge for beam time at ESRF on the CRG-IF beam line, technical support of the beam line staff and stimulating discussion with Y. Gauthier.

*Corresponding author. Email address: desantis@labs.polycnrs-gre.fr

[1] C.-J. Lin and G. L. Gorman, Appl. Phys. Lett. **61**, 1600 (1992).
[2] D. Weller, H. Brändle, and C. Chappert, J. Magn. Magn. Mater. **121**, 461 (1993).
[3] G. R. Harp, D. Weller, T. A. Rabedeau, R. F. Farrow, and M. F. Toney, Phys. Rev. Lett. **71**, 2493 (1993).
[4] D. Weller, H. Brändle, and C. Chappert, J. Magn. Magn. Mater. **121**, 461 (1993).
[5] T. B. Massalski, *Binary Alloy Phase Diagrams*, 2nd ed. (ASM International, Materials Park, Ohio, 1993), Vol. 2, pp. 1225, 1752.
[6] J. M. Sanchez, J. L. Morán-López, C. Leroux, and M. C. Cadeville, J. Phys.: Condens. Matter **1**, 491 (1989).
[7] M. Maret, M. C. Cadeville, W. Staiger, E. Beaurepaire, R. Poinsot, and A. Herr, Thin Solid Films **275**, 224 (1996).
[8] P. W. Rooney, A. L. Shapiro, M. Q. Tran, and F. Hellerman, Phys. Rev. Lett. **75**, 1843 (1995).
[9] A. L. Shapiro, P. W. Rooney, M. Q. Tran, F. Hellman, K. M. Ring, K. L. Kavanagh, B. Rellinghaus, and D. Weller, Phys. Rev. B **60**, 12 826 (1999).
[10] Y. Gauthier, R. Baudoing-Savois, J. J. W. M. Rosink, and M. Sotto, Surf. Sci. **297**, 193 (1993).
[11] S. Ferrer, P. Fajardo, F. De Bergevin, J. Alvarez, X. Torrelles, H. A. van der Vegt, and V. H. Etgens, Phys. Rev. Lett. **77**, 747 (1996).
[12] Y. Gauthier, R. Baudoing-Savois, J. M. Bugnard, U. Bardi, and A. Atrei, Surf. Sci. **276**, 1 (1992).
[13] T. A. Tyson, S. D. Conradson, R. F. C. Farrow, and B. A. Jones, Phys. Rev. B **54**, R3702 (1996).
[14] C. Meneghini, M. Maret, M. C. Cadeville, and J. L. Hazemann, J. Phys. IV **7**, C2-1115 (1997).
[15] J. L. Hazemann, K. Nayouf, and F. De Bergevin, Nucl. Instrum. Methods Phys. Res. B **97**, 547 (1995).
[16] R. Baudoing-Savois, G. Renaud, M. De Santis, A. Barbier, O. Robach, P. Taunier, P. Jeantet, O. Ulrich, J. P. Roux, M. C. Saint-Lager, A. Barski, O. Geaymond, G. Berard, P. Dolle, M. Noblet, and A. Mougin, Nucl. Instrum. Methods Phys. Res. B **149**, 213 (1999).

[17] R. Kunkel, B. Poelsema, L. K. Verheij, and G. Comsa, Phys. Rev. Lett. **65**, 733 (1990).
[18] M. C. Saint-Lager, R. Baudoing-Savois, M. De Santis, P. Dolle, and Y. Gauthier, Surf. Sci. **418**, 485 (1998).
[19] G. Grübel, K. G. Huang, D. Gibbs, D. M. Zehner, A. R. Sandy, and G. J. Mochrie, Phys. Rev. B **48**, 18 119 (1993).
[20] E. Vlieg, J. Appl. Crystallogr. **33**, 401 (2000).
[21] E. Vlieg, J. Appl. Crystallogr. **31**, 198 (1998).
[22] R. Feidenhans'l, Surf. Sci. Rep. **10**, 105 (1989).
[23] D. T. Cromer and D. A. Liberman, Acta Crystallogr., Sect. A: Cryst. Phys., Diffr., Theor. Gen. Crystallogr. **37**, 267 (1981).
[24] E. Weschke, C. Schüßler-Langeheine, R. Meier, G. Kaindl, C. Sutter, D. Abernaty, and G. Grübel, Phys. Rev. Lett. **79**, 3954 (1997).
[25] I. K. Robinson, Phys. Rev. B **33**, 3830 (1986).
[26] S. Ferrer, J. Alvarez, E. Lundgren, X. Torrelles, P. Fajardo, and F. Boscherini, Phys. Rev. B **56**, 9848 (1997).
[27] *International Tables for X-ray Crystallography* (Kynoch Press, Birmingham, U.K., 1968), Vol. III.
[28] C. Leroux, M. C. Cadeville, V. Pierron-Bohnes, G. Inden, and F. Hinz, J. Phys. F: Met. Phys. **18**, 2033 (1988).
[29] U. Bardi, Rep. Prog. Phys. **57**, 939 (1994).
[30] S. Gallego, C. Ocal, M. N. Muñoz, and F. Soria, Phys. Rev. B **56**, 12 139 (1997).
[31] M. De Santis, R. Baudoing-Savois, P. Dolle, M. C. Saint-Lager, and Y. Gauthier, Surf. Rev. Lett. **6**, 361 (1999).
[32] H. Berg and J. B. Cohen, Metall. Trans. **3**, 1797 (1972).
[33] M. Galeotti, A. Atrei, U. Bardi, B. Cortigiani, G. Rovida, and M. Torrini, Surf. Rev. Lett. **3**, 1691 (1996).
[34] J. M. Roussel, A. Saul, G. Treglia, and B. Legrand, Phys. Rev. B **55**, 10 931 (1997).
[35] A. Christensen, A. V. Ruban, P. Stoltze, K. W. Jacobsen, H. L. Skriver, J. K. Nørskov, and F. Besenbacher, Phys. Rev. B **56**, 5822 (1997).
[36] S. Rousset, S. Chiang, D. E. Fowler, and D. D. Chambliss, Phys. Rev. Lett. **69**, 3200 (1992).
[37] C. T. Chan, K. B. Bohnen, and K. M. Ho, Phys. Rev. Lett. **69**, 1672 (1992).
[38] P. W. Murray, S. Thorshaug, I. Stensgaard, F. Besenbacher, E. Lægsgaard, A. Ruban, K. W. Jacobsen, G. Kopidakis, and H. L. Skriver, Phys. Rev. B **55**, 1380 (1997).
[39] P. Gambardella and Klaus Kern, Surf. Sci. **475**, L229 (2001).
[40] E. Lundgren, B. Stanka, M. Schmid, and P. Varga, Phys. Rev. B **62**, 2843 (2000).
[41] N. W. E. McGee, M. T. Johnson, J. J. de Vries, and J. aan de Stegge, J. Appl. Phys. **73**, 3418 (1993).
[42] P. Bruno, G. Bayreuther, P. Beauvillain, C. Chappert, G. Luggert, D. Renard, J. P. Renard, and J. Seiden, J. Appl. Phys. **68**, 5759 (1990).
[43] C. S. Shern, J. S. Tsay, H. Y. Her, Y. E. Wu, and R. H. Chen, Surf. Sci. **429**, L497 (1999).
[44] F. Cadegnani, thesis, University of Modena, Italy.